Cell, Vol. 113, 767–776, June 13, 2003, Copyright ©2003 by Cell Press

Control of Cell Morphogenesis in Bacteria: Two Distinct Ways to Make a Rod-Shaped Cell

Richard A. Daniel and Jeff Errington*
Sir William Dunn School of Pathology
University of Oxford
Oxford OX1 3RE
United Kingdom

Summary

Cell shape in most eubacteria is maintained by a tough external peptidoglycan cell wall. Recently, cell shape determining proteins of the MreB family were shown to form helical, actin-like cables in the cell. We used a fluorescent derivative of the antibiotic vancomycin as a probe for nascent peptidoglycan synthesis in unfixed cells of various Gram-positive bacteria. In the rod-shaped bacterium *B. subtilis*, synthesis of the cylindrical part of the cell wall occurs in a helical pattern governed by an MreB homolog, Mbl. However, a few rod-shaped bacteria have no MreB system. Here, a rod-like shape can be achieved by a completely different mechanism based on use of polar growth zones derived from the division machinery. These results provide insights into the diverse molecular strategies used by bacteria to control their cellular morphology, as well as suggesting ways in which these strategies may impact on growth rates and cell envelope structure.

Introduction

Bacteria exist in a wide variety of shapes and, historically, cell morphology has been an important taxonomic criterion. In eubacteria, the peptidoglycan (PG) layer of the cell wall is a major determinant of cell shape. It is built from long glycan strands crosslinked by short peptides. The resultant meshwork structure comprises a single huge molecule (the sacculus) that covers the whole surface of the cell (reviewed by Foster and Popham, 2001; Höltje, 1998). When the PG layer is stripped from cells in a more or less intact form, the layer retains the shape of the organism from which it was obtained. Moreover, many genes that when mutated, lead to an altered cell shape (morphogenes), encode products involved in PG synthesis. Nevertheless, how the three-dimensional shape of the organism specified by its genes is imposed on assembly of the wall sacculus remains poorly understood. Recently, an important step forward was taken when it emerged that a broadly conserved morphogene, *mreB*, encodes an actin homolog that can assemble into helical cables that could comprise cytoskeletal elements with a direct role in cell shape determination (Jones et al., 2001; van den Ent et al., 2001; Carballido-López and Errington, 2003). *B. subtilis* (not unusually) actually has three MreB family proteins, and two of these proteins, arbitrarily called MreB and Mbl (*MreB-l*ike), seem to cooperate in determining cell shape. The relative roles of these closely-related proteins are partially resolved in this paper.

The precursor for PG synthesis is a disaccharide pentapeptide that is synthesized in the cytosol and then transferred to the outside of the cytoplasmic membrane. Here, penicillin binding proteins (PBPs) add precursors to the existing high molecular weight PG by a combination of transglycosylation and transpeptidation reactions. These reactions have been extensively characterized (Goffin and Ghuysen, 1998; Höltje, 1998) and are targets for important antibiotics—the β-lactams (e.g., penicillins) inhibit transpeptidation, and the glycopeptides inhibit transglycosylation. Vancomycin, an example of the latter class, is the last line of defense against certain hospital infections. Precisely how it blocks transglycosylation remains unclear, but it is known that it binds tightly to the terminal D-Ala-D-Ala of the PG precursor (Sheldrick et al., 1978).

A crucial question that follows from the discovery of the MreB cytoskeleton lies in how these cytoskeletal cables control the topology of PG synthesis. In principle, they might act by localizing one or more of the enzymes involved in precursor synthesis, delivery of the precursor to the surface, or incorporation of the precursor into the sacculus. However, previous work with the rod-shaped bacteria *E. coli* and *B. subtilis* has revealed that PG synthesis occurs in a relatively dispersed manner, all over the cylindrical part of the cell (Burman et al., 1983; Clarke-Sturman et al., 1989; de Pedro et al., 1997; Merad et al., 1989; Mobley et al., 1984; Schlaeppi et al., 1982; Wientjes and Nanninga, 1989; Woldringh et al., 1987). Another aspect of this spatial problem lies in the way that the individual glycan strands are organized within the sacculus. Again, this is poorly understood. Individual glycan strands have a heterogeneous length up to a maximum of about 100 disaccharide units (reviewed by Höltje, 1998). A polymer of this length would be much too short to encircle the diameter of a typical cell. In principle, the glycan strands could be inserted randomly to form an amorphous mat, or they could be inserted at a specific angle relative to the long axis of the cell (reviewed by Koch, 1988). A third aspect of the spatial organization of the PG layer relates to its thickness. In Gram-negative bacteria, the layer is thin, perhaps comprising a two-dimensional network. In Gram-positive bacteria, the PG layer is thick, with presumably an extra dimension of crosslinks between layers. There is good evidence that in these organisms, growth of the cylindrical part of the wall occurs by insertion of new material at the surface of the cytoplasmic membrane (Merad et al., 1989; Mobley et al., 1984; Pooley, 1976a, 1976b). This material is probably incorporated in a non-load-bearing, relaxed state. As new layers of material are inserted below, the older material migrates outward and becomes increasingly stretched until it reaches the surface of the cell and becomes load bearing. Autolytic action at the cell surface then hydrolyses the material to allow continued cell enlargement (Doyle et al., 1988).

Understanding the molecular basis for cell shape determination has been hampered by the lack of sensitive

*Correspondence: jeff.errington@path.ox.ac.uk

and high-resolution probes for nascent PG synthesis in unfixed cells. Vancomycin is a clinically important antibiotic that binds to the terminal D-Ala-D-Ala of peptidoglycan. In most bacteria, these termini should be rapidly protected from vancomycin binding by processing, either through the formation of crosslinks or through hydrolysis by carboxypeptidases (Höltje, 1998). We reasoned that vancomycin should bind specifically to nascent PG and, therefore, that fluorescent derivatives of vancomycin might provide sensitive tools for probing the topology of PG synthesis. Here, we describe the use of a fluorescent derivative of vancomycin (Van-FL) to probe the pattern of insertion of nascent wall material by fluorescence microscopy. We show that distinct and reproducible patterns of staining can be obtained with several different Gram-positive bacteria (Gram-negative bacteria do not stain because their outer membrane presents a permeability barrier to this drug; Vuorio and Vaara, 1992). In each case, the pattern probably reveals details of nascent PG synthesis at high resolution in unfixed cells. In *B. subtilis*, the label visualizes a helical pattern of nascent PG synthesis in the cylindrical part of the cell, as well as the expected intense staining at active or recent division sites. The helical pattern is reminiscent of the helical cables formed by both MreB and Mbl proteins in this organism (Jones et al., 2001). The helical pattern, but not division-associated staining, was abolished by elimination of Mbl protein, but not MreB. These results have several important implications; they show that the insertion of new wall material in the *B. subtilis* cylinder occurs in a helical manner, that Mbl is the MreB homolog required for this insertion, and that in the absence of Mbl, *B. subtilis* probably survives by switching to a polar or cell-division-directed mode of growth. In a rod-shaped bacterium with no MreB/Mbl system (*Corynebacterium glutamicum*) shape is achieved by polar growth, similar to *mbl* mutants of *B. subtilis*. The results provide insights into the topological organization of cell wall synthesis in bacteria and into the molecular basis for differences in wall growth and cell shape in diverse bacteria.

Results

Use of Van-FL to Stain Sites of Nascent Cell Wall Synthesis in *B. subtilis*

Vancomycin binds to the terminal D-Ala-D-Ala found on PG precursors or inserted precursor that has not been involved in the formation of a crosslink (reviewed by Reynolds, 1989). The binding inhibits transpeptidase activity directly, but secondary direct or indirect effects on transglycosylation have also been reported (Ge et al., 1999). This mode of binding suggested that labeled vancomycin might provide a stain for nascent PG synthesis. If so, we could test whether the topology of insertion of PG is controlled by the helical cables of MreB and/or Mbl. Vancomycin labeled with fluorescein on its only amide group (Van-FL) was used to stain exponentially growing cells of wild-type *B. subtilis*. A highly reproducible pattern was observed. Figure 1A shows a compilation of closeups of typical cells of different lengths. The most prominent staining occurred in broad bands that appeared to correspond to division sites (arrows).

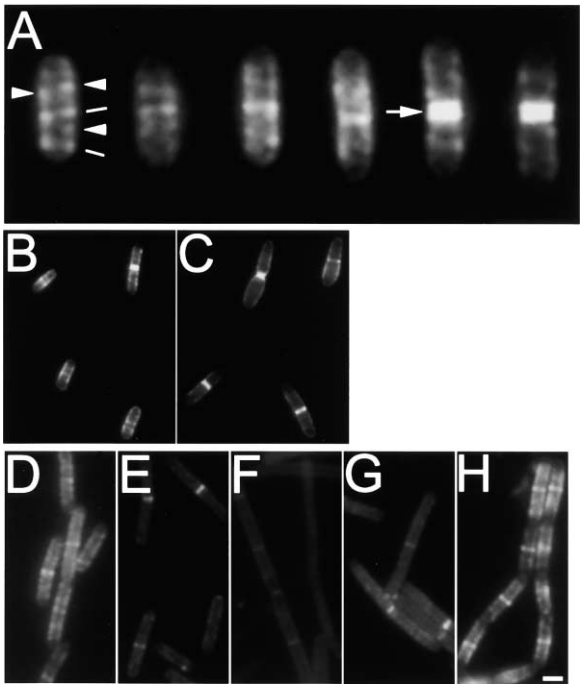

Figure 1. Van-FL Staining of *B. subtilis* Cells and the Effects of Inhibitors of PG Precursor Synthesis and Incorporation

(A) Compilation of wild-type cells (strain 168) stained with Van-FL, arranged (left to right) approximately according to cell cycle progression. The arrow points to a densely stained region representing a division site. Lines and arrowheads indicate tilted bands and peripheral dots, respectively, that are characteristic of a helical mode of staining.

(B and C) Strain 853 grown in the presence (B) or absence (C) of IPTG, the inducer of *murE* operon expression.

(D–H) Stained cells of the wild-type (strain 168) after treatment with no agent (D), 0.05% sodium azide (E), 200 μg/ml bacitracin (F), 500 μg/ml phosphomycin (G), or 100 μg/ml penicillin G (H). Scale bar = 2 μm.

This was consistent with the massive PG synthesis expected to occur during division, when a thick new layer of PG is formed rapidly at this site. The staining appeared to be associated with nascent or newly formed division septa, because short cells in which division would have recently occurred sometimes exhibited a single labeled pole, whereas older cells showed little or no polar staining. The general lack of polar staining was expected because various experimental approaches have shown that once the cell poles have been formed, they undergo very little wall turnover in either *B. subtilis* or *E. coli* (e.g., Clarke-Sturman et al., 1989; de Pedro et al., 1997; Mobley et al., 1984; Schlaeppi et al., 1982).

Less prominent but clearly visible staining was detected in the cylindrical parts of all of the cells. Careful inspection of this staining highlighted the frequent presence of bands slanted relative to the long axis of the cell (lines in Figure 1A) and prominent dots near the cell periphery (arrowheads). This pattern was reminiscent of the helical pattern produced by cells stained for MreB and Mbl (Jones et al., 2001). The peripheral dots arise because the helix is closest to being perpendicular to the image plane and, therefore, brightest at the edge of the cell. Three-dimensional image reconstructions were

technically demanding because of bleaching and the weak signal-to-noise ratio. However, in the 3D representation shown in Supplemental Figure S1 (online at http://www.cell.com/cgi/content/full/113/6/767/DC1), weak tilted bands of fluorescence could be discerned joining some of the strong peripheral dots, consistent with the pattern reflecting a helical stain.

Van-FL Staining Requires Active Synthesis and Externalization of PG Precursors

It was important to confirm that Van-FL was indeed staining sites of nascent peptidoglycan synthesis. If so, the staining should be dependent on ongoing PG synthesis. To test this, the effects of various inhibitors of PG precursor synthesis and incorporation were examined. The *murE* gene encodes UDP-N-acetylmuramyl tripeptide synthetase, one of the earlier steps in precursor synthesis (Michaud et al., 1990). The gene is essential, so we constructed a strain in which the expression of the *mur* operon (Daniel and Errington, 1993; Henriques et al., 1992) was conditional on the presence of IPTG. In cells from a culture grown in the presence of IPTG, cell morphology was normal, and the staining pattern was indistinguishable from that of wild-type *B. subtilis* (Figure 1B). When IPTG was removed, after a period of time during which MurE protein (and probably other gene products from the PG precursor synthetic pathway operon; MraY, MurD, MurG, and MurB) was depleted, the cells began to develop a swollen and lytic appearance, presumably due to the reduction of wall synthesis, but continued autolytic activity. These cells showed a corresponding clear reduction in overall Van-FL staining. The residual staining evident, particularly at division sites, was presumably due to residual MurE activity. Chemical inhibitors of precursor synthesis had a much more rapid effect. A control untreated culture is illustrated in Figure 1D. A general inhibitor of metabolism, sodium azide greatly reduced staining (Figure 1E) as expected, as did more specific inhibitors of PG precursor synthesis bacitracin (Figure 1F) and phosphomycin (Figure 1G). Cycloserine had a similar effect (data not shown). Phosphomycin acts at a very early step in precursor synthesis, formation of N-acetyl-muramic acid, whereas bacitracin acts late, in recycling of the lipid carrier (Stone and Strominger, 1971).Thus, staining was dependent on PG precursor synthesis. Presumably, it is also dependent on precursor transport because vancomycin is a large (MW 1485.7), hydrophilic molecule that is specific for Gram-positive bacteria because it can not cross the outer membrane of Gram-negative bacteria (Vuorio and Vaara, 1992). In contrast, penicillin G, which specifically inhibits the crosslinking of PG, had little effect on the staining pattern (Figure 1H). These results were consistent with the target of vancomycin labeling being externalized PG precursors.

Fluorescent Vancomycin Probably Stains Unincorporated Lipid-Linked PG Precursors on the Cell Surface

To determine the location of the Van-FL staining, cells were treated with lysozyme, to release label attached to material covalently associated with the cell wall, or with detergent, to release label associated with the membrane. As shown in Table 1, top, very little label was released from cells treated with lysozyme to release label attached to material covalently associated with the cell wall or with detergent to release label associated with the membrane. Treatment with detergent alone released about 50% of the label (Table 1, bottom). The remaining label was still only slightly solubilized by lysozyme treatment, but again, after lysozyme treatment, most of the label could be released by detergent. These results suggested that about half of the Van-FL is associated with PG precursor in the externalized but unincorporated "lipid II" form, and the other half is covalently associated with the PG layer but still membrane associated and, therefore, located at the growing end of the glycan strand. On the basis of these results and previous work on the mode of action of vancomycin, it appears that Van-FL stains sites that are involved in nascent PG synthesis.

Table 1. Release of Van-FL by Lysozyme or Detergent Treatments

Treatment	Vancomycin Released into Supernatant (% Total)
Lysozyme→Detergent	
PBS wash	0.1 (±1.6)
Lysozyme	11 (±3.2)
PBS wash	4.6 (±2.1)
Detergent	75 (±3.4)
Detergent→Lysozyme	
PBS wash	2 (±1.2)
Detergent	45 (±2.5)
Lysozyme	8 (±4.3)
Detergent	37 (±4.0)

Separate Systems for Septal and Cylindrical PG Synthesis in *B. subtilis*

If the bright midcell bands and fainter helical sidewall staining represented the distinct insertion of new PG at sites of cell division and the cell cylinder, mutations specifically blocking these pathways should have predictable effects on the staining pattern. As shown in Figure 2, depletion of the essential cell division proteins FtsZ (early acting; Figure 2A) and PBP 2B (late acting; Figure 2B) both eliminated the septal staining pattern (Daniel et al., 2000), but the helical pattern remained and extended more or less throughout the filamentous cells. This confirmed that the prominent medial and sometimes polar staining was dependent on cell division.

Mbl, but Not MreB, Is Required for the Helical Pattern of Sidewall Staining

We previously showed that the morphogenic proteins MreB and Mbl both form helical structures running around the periphery of the *B. subtilis* cell cylinder (Jones et al., 2001). Either or both of these proteins could be responsible for the helical staining pattern described above. The *mreB* gene is essential, but we previously reported the construction of a conditional mutant that can be grown in the presence of an inducer xylose. When the *mreB* gene is repressed by removal of xylose, the cells become bloated and eventually lyse (Jones et

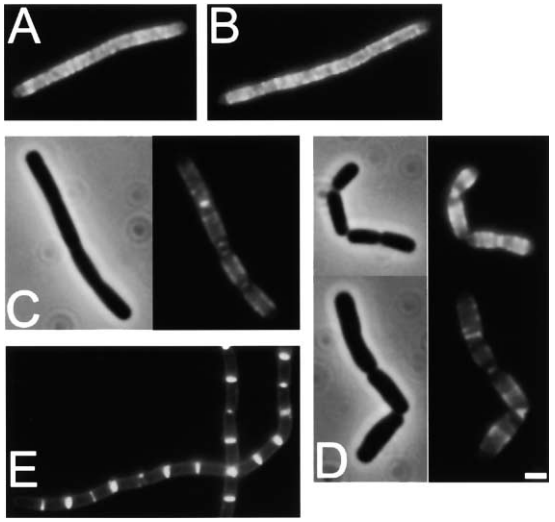

Figure 2. Effects of Morphogenic Mutations on Van-FL staining

B. subtilis strains bearing mutations affecting various morphogenic processes were stained with Van-FL. (A and B) Cell division mutants. Strains 1801 and 3295 were grown in the absence of IPTG to deplete essential cell division proteins FtsZ (A) and PBP 2B (B). (C and D) Strain 2060, allowing repression of the *mreB* gene, was grown in the presence (C) and absence (D) of xylose. (E) Strain 2505, carrying a null mutation in the *mbl* gene. Scale bar = 2 μm.

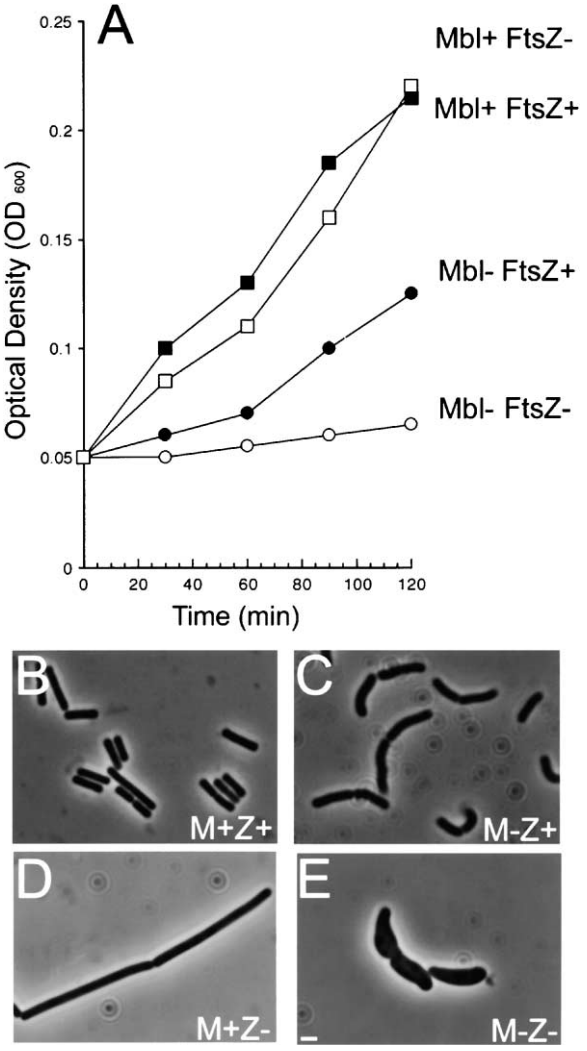

Figure 3. Dependence of Growth of *mbl* Mutant Cells on Cell Division

(A) Isogenic *mbl*$^+$ (strain 1801; squares) and *mbl* mutant (strain 3296; circles) strains containing an IPTG-inducible *ftsZ* allele were grown in the presence of inducer, then diluted back into media with (closed symbols) or without (open symbols) IPTG. Samples were taken to follow growth (OD_{600}) at the time intervals shown.

(B–E) At the end of the experiment, samples were taken from each culture for examination by phase contrast microscopy. (B) *mbl*$^+$ +IPTG. (C) *mbl* +IPTG. (D) *mbl*$^+$ −IPTG. (E) *mbl* −IPTG. Scale bar = 2 μm.

al., 2001). Figure 2C shows that in the presence of xylose, the cells had a normal morphology and they exhibited the typical Van-FL staining pattern. After growth in the absence of xylose, the cells became wider and bloated, illustrating the dependence on MreB for control of cell width, but in most cells a helical or circumferential staining remained visible over much of the cell surface (Figure 2D). On this basis, it appears that MreB is not absolutely required for the helical pattern, though we could not exclude a qualitative effect on the pattern.

The *mbl* gene is not essential but null mutants grow slowly and have a twisted and sometimes bloated phenotype (Abhayawardhane and Stewart, 1995; Jones et al., 2001). Surprisingly, in the absence of Mbl protein, the distinct helical Van-FL staining pattern in the side walls was virtually eliminated (Figure 2E). Further, the staining at division sites was not only retained, but it also appeared much brighter than usual, and the bands were broader. The loss of the helical staining pattern in the absence of Mbl provided strong support for the notion that the helical cables made by this actin homolog are primarily responsible for the helical pattern of vancomycin staining and, therefore, for the presumptive helical insertion of nascent peptidoglycan. This result also, surprisingly, suggested that it is Mbl protein, rather than MreB, that is primarily responsible for cylindrical wall synthesis.

On the basis of these findings, both the slowness and nonlinearity of growth of *mbl* mutants could be due to the loss of ability to undergo significant expansion of the cylindrical part of the cell wall, leaving only growth from polar zones generated by cell division. To test this idea, we tried to construct strains in which the *mbl* null mutation was combined with conditional mutations in several different cell division genes, including *ftsZ*, *divIB*, and *pbpB*. The genetic analysis was complicated by the ready accumulation of mutations that improve the growth of *mbl* mutants, which have been reported previously (Abhayawardhane and Stewart, 1995). Nevertheless, the various double mutants constructed all showed a much more severe growth defect under conditions partially permissive for the division defect. We succeeded in constructing a strain with a disruption of *mbl* and an IPTG-inducible *ftsZ* gene (strain 3296). Figure 3C shows that in the presence of IPTG, this strain had a typical Mbl mutant phenotype, with twisted cells and some loss of width control. As expected, the growth rate of this strain was reduced about 2-fold compared

with the isogenic *mbl*$^+$ strain (Figure 3A), which showed a normal cell morphology (Figure 3B). In the absence of IPTG, the *mbl*$^+$ strain showed the expected block in cell division, leading to the formation of elongated filamentous cells (Figure 3D), but the overall growth rate of the culture was not affected (Figure 3A). However, the *mbl* mutant strain showed an almost complete arrest in growth in the absence of IPTG, and microscopic examination of the cells showed that they had remained relatively short and had become much more bloated. These observations strongly supported the view that the *mbl* mutant was unable to grow via extension of the cell cylinder and was relying on localized growth zones dependent on the division machinery.

Diverse Patterns of Van-FL Staining in Other Gram-Positive Bacteria

The staining results with *B. subtilis* were all consistent with the Van-FL labeling sites of nascent PG synthesis. Since vancomycin is active against a wide range of bacteria, it should be possible to use Van-FL to stain other Gram-positive bacteria to probe their cell wall growth properties. Various streptococci have been studied in detail previously. These spherical cells synthesize wall material specifically from equatorial rings that elongate and constrict to bring about cell division (reviewed by Koch, 2000). Consistent with expectation, *S. pneumoniae* cells showed very light staining over most of their ovoid surface, but developing invaginations between sister cells contained brightly stained bands (arrows in Figure 4A). Furthermore, large ovoid cells that were presumably preparing for their next division, but not always with detectable invaginations, often contained midcell bands of staining (arrowheads).

S. coelicolor is a Gram-positive bacterium from the high G + C group, distinct from the low G + C *Bacillus/Clostridium* group. It has a branching mycelial growth habit. Light microscopical observations have suggested that this organism grows specifically from the tips of the elongating hyphae (Gray et al., 1990). Presumably, dispersed cylindrical growth would be incompatible with the three-dimensional restraints exerted by the branched overlapping hyphae. Spores of *S. coelicolor* were allowed to outgrow and then stained with Van-FL, using the same protocol as for *B. subtilis*. As shown in Figure 4B, the hyphae showed bright staining at the tips of the hyphae, as well as at occasional intermediate sites that appeared to correspond to newly forming branch sites. The cylindrical parts of the hyphae between tips and septa were unstained. These results provided strong evidence to support the notion that Van-FL staining faithfully identifies the sites of PG synthesis in Gram-positive bacteria.

An MreB-Independent Way to Form a Rod-Shaped Bacterium

We previously reported an interesting correlation between posession of at least one copy of *mreB* and a noncoccoid (round) cell shape (Jones et al., 2001). Now that nearly 100 bacterial genomes have been completely sequenced, it is possible to do a comprehensive survey of the distribution of *mreB* across a wide range of bacterial taxa relative to their shape. Supplemental Table S1

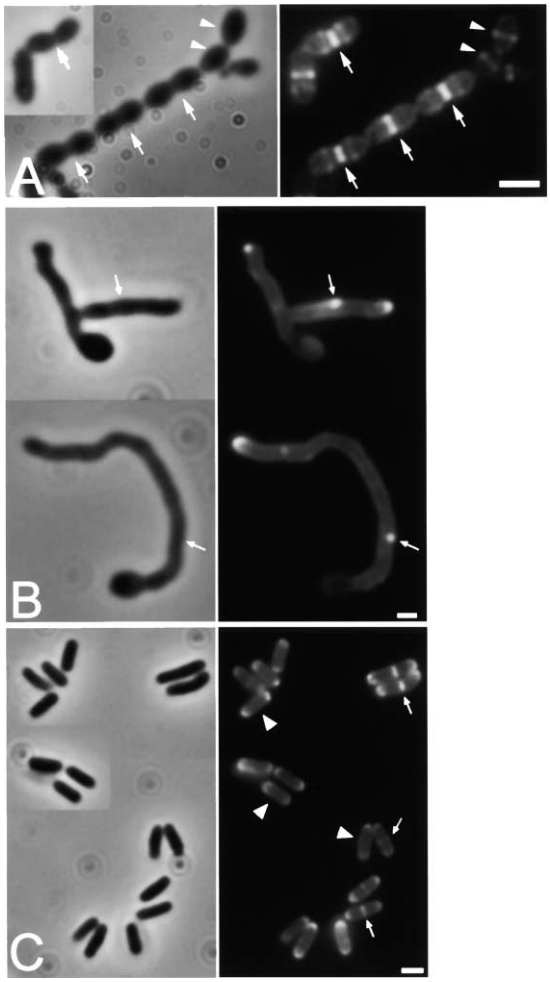

Figure 4. Distinct Van-FL Staining Patterns for *Streptococcus*, *Streptomyces*, and *Corynebacterium* Cells

Left shows phase contrast images and, right, corresponding fluorescence images. Scale bars = 2 μm. (A) *S. pneumoniae* R6. Arrows indicate deeply constricted, heavily stained zones. Arrowheads indicate lightly staining medial bands, presumably corresponding to new growth zones that will become division sites. (B) *S. coelicolor* M145. Arrowheads indicate subapical spots of staining that probably represent nascent branch points. (C) *Corynebacterium glutamicum*. The cells to the right are undergoing division and have a prominent band of transverse staining at their midpoint. To the left, the cells are not yet dividing but appear to have nascent wall synthesis at both cell poles.

(online at http://www.cell.com/cgi/content/full/113/6/767/DC1) shows the results of such a survey, and Table 2 summarizes the results in the context of a recent representation of the phylogenetic tree of the eubacteria (Prescott et al., 1999). The tree shows that *mreB* homologs are present all around the eubacterial kingdom, including some of the most deeply rooted species such as *Aquifex* and *Thermotoga*. This suggests that MreB is an ancient protein, probably present in the last common ancestor of the eubacteria. Most of these lineages contain rod-shaped bacteria. However, the MreB gene has been lost from several of the lineages, likely representing a series of independent events. Most spherical organisms (cocci) are found in lineages that have lost (or do

Table 2. Phylogenetic Distribution of MreB Proteins in the Eubacteria and Its Relationship with Cell Shape[a]

Phylogeny	Number of Organisms in Class[b]			
	Nonround		Round	
	MreB$^+$	MreB$^-$	MreB$^+$	MreB$^-$
(Archaea)				
Aquifex	1	0	0	0
Thermotogas	1	0	0	0
Green nonsulfur bacteria	0	0	0	0
Deinococci	0	0	0	1
Low G + C Gram + ve	10	5[c]	0	6
High G + C Gram + ve	1	6[d]	0	0
β−Proteobacteria	1	0	0	1
γ−Proteobacteria	16	1	0	0
α−Proteobacteria	3	6[d]	0	0
ϵ−Proteobacteria	2	0	0	0
δ−Proteobacteria	0	0	0	0
Spirochaetes	3	0	0	0
Cyanobacteria	2	0	1[e]	0
Planctomycetes	0	0	3[e]	0
Bacteroides/Chlorobi group	2	0	0	0
Totals	42	18	4	8

[a] Phylogenetic layout taken from Prescott et al. (1999).
[b] Data derived from Table S1 (online at http://www.cell.com/cgi/content/full/113/6/767/DC1).
[c] *Mycoplasmas*. These are pleiomorphic, wall-less organisms with a range of unconventional cytoskeletal elements.
[d] *Corynebacterium/Mycobacterium* group and *Agrobacterium/Rhizobium* group. Slow growing rod-shaped organisms with no MreB homologues.
[e] These organisms have MreB and are often spherical but, in at least some cases, have differentiated forms that might require an MreB cytoskeleton.

not possess) MreB: e.g., *Staphylococcus, Streptococcus, Lactococcus* (Low G + C Gram positives), *Neisseria* (β-proteobacteria), and *Deinococcus*. The exceptions that are round but possess MreB comprise some cyanobacteria and the chlamydia (Planctomycetes) (see footnote d in Table 2). These organisms have in common the ability to undergo morphological differentiation, which might provide a function for MreB.

Although many bacteria with nonround shapes have at least one copy of MreB, there are now three major groups of bacteria that clearly do not. The Mycoplasmas (see footnote b in Table 2) can be considered a special case because they are very specialized wall-less organisms in which shape is apparently controlled by a diversity of cytoskeletal proteins that are in general, unconventional and poorly conserved (Trachtenberg, 1998). However, the other two groups, both comprising rod-shaped organisms, are common bacteria found in a wide range of habitats (see footnote c in Table 2): Gram-negative α-proteobacteria of the class *Rhizobium*, which includes important plant symbionts and pathogens (e.g., *Mesorhizobium* and *Agrobacterium*), and several high G + C, Gram-positive bacteria (*Actinobacteria*), particularly Corynebacteria and Mycobacteria. How can these groups of bacteria achieve a rod-like shape in the absence of MreB? Given our data with the *mbl* mutant and the results with *Streptomyces*, we considered the possibility that these organisms exhibit polar growth from zones specified initially by the division machinery but which are not shut down after division as they normally are in *Bacillus*. Electron microscopical examination of *Corynebacterium diphtheriae* stained with antiserum against total wall material had suggested that this organism does indeed exhibit apical growth, as for *Streptomyces* (Umeda and Amako, 1983). To confirm this for a sequenced organism with no *mreB* gene, we grew *Corynebacterium glutamicum* and stained the cells with Van-FL. Typical results are shown in Figure 4C. Several longer cells to the right of the panel, apparently about to divide, showed staining both at their poles and in prominent bands at mid cell. The shorter, nondividing cells to the left had bright staining at their poles, but the cylinders were poorly stained. This pattern was strikingly different from that of wild-type *B. subtilis* in which the cell cylinder was stained but the poles were inert (Figure 1A). The simplest interpretation of the *Corynebacterium* pattern is that newborn cells have growth zones at both poles, and that cell growth gives rise to an elongating tube of inert wall material bounded by active cell poles. After roughly doubling in cell length, the division machinery initiates the formation of a new division septum. Unlike *B. subtilis*, in which wall synthesis at the division site is shut down after the new cell poles are formed, in *Corynebacterium*, the synthetic machinery remains active and cell elongation occurs, perhaps indefinitely, from the two new cell poles. Thus, although the gross cell morphology of *Corynebacterium* is rather similar to that of *Bacillus*, the two bacteria achieve this morphology by quite different growth strategies.

Discussion

Van-FL as a Probe for Nascent PG Synthesis in Bacteria

A number of approaches have been used to visualize the localization of nascent PG synthesis in bacterial

cells. Most methods based on electron microscopy rely on thin sectioning (e.g., Merad et al., 1989), which means that the overall topology of insertion across the cell surface is difficult to determine. De Pedro et al. (1997) have described an elegant approach in which D-Ala was replaced with D-Cys, which could be visualized by use of chemical agents that bind to the thiol group. However, this can only be used on isolated sacculi that have been deproteinized. We reasoned that Van-FL might provide a means of visualizing the sites of PG synthesis in unfixed cells, since it is known to bind to the terminal D-Ala-D-Ala of the lipid-linked PG precursor (Sheldrick et al., 1978). The antibiotic cannot penetrate the cell membrane, so it should only bind to externalized precursor or to the recently inserted lipid-linked subunit at the growing end of a glycan strand. Although the staining could be influenced by a number of factors, particularly the activity of carboxypeptidases that remove D-Ala-D-Ala (Höltje, 1998), several lines of evidence suggest that Van-FL staining does indeed provide important information on the localization of nascent PG synthesis. First, direct cell fractionation methods showed that much of the Van-FL could be released partly by detergent action and almost all by a combination of detergent and lysozyme (Table 1). Second, the staining was greatly reduced by various treatments that inhibit the supply of PG precursor synthesis. Third, several other Gram-positive bacteria that were examined gave staining patterns that were consistent with predictions. Finally, when mutants affected in septal (*ftsZ*, *pbpB*) or cylindrical (*mreB*, *mbl*) cell wall synthesis were examined in the three cases where an effect was seen, specific loss of the expected element of the staining pattern occurred. We conclude that Van-FL staining provides a powerful tool to study the topology of PG synthesis in Gram-positive bacteria.

Helical Insertion of Nascent PG Synthesis in *B. subtilis*

Previous studies of the topology of PG synthesis in *B. subtilis* have led to the conclusion that new material is inserted in a diffuse manner all over the cylindrical surface of the cell (reviewed by Archibald et al., 1993). However, this early work, based mainly on transmission electron microscopy of thin sections, probably did not provide the three-dimensional resolution needed to detect helical insertion. The discovery that PG is actually inserted in a helical manner has important implications for growth of the cell wall. If the helix directing cell wall synthesis were statically positioned it would be difficult to see how uniform growth of the cell wall cylinder could be achieved. However, we have recently shown that the Mbl cables undergo continuous increase in length, in parallel with cell length extension, but that the helical pitch of the cables is more or less maintained (Carballido-López and Errington, 2003). Unless all growth occurs at the cell poles (which this and previous work excludes), this means that the helical cables must sweep across the surface of the cell as it grows. Furthermore, stretching of the preexisting PG layer to allow elongation of the cell is likely to generate a rotational torque in the direction of unwinding of the helix. This opposite rotation would contribute further to movement of the helical cables relative to the cell surface, facilitating a complete sweep of the surface of the cell with new PG during each doubling in cell length. Consistent with this idea, Mendelson and coworkers, and Koch, have noted that the growth of *B. subtilis* cells is actually accompanied by a helical rotation of one cell end relative to the other. It was not clear whether this was due to a helical form of synthesis (Mendelson, 1976) or was a consequence of the combination of longitudinal and radial stresses incurred in the wall during cell elongation (Koch, 1990). Our results provide a mechanism that directly explains the helical growth of the cell. Formally, it was possible that the helical cables of MreB and Mbl act as a brace that maintains the cylindrical shape of the cell while diffuse synthesis takes place all over the surface. The Van-FL staining probably excludes this model and provides strong support for the view that the cables of Mbl, at least, actively direct the synthesis of new PG in a spatially controlled manner.

Mbl Protein Is Specialized in the Control of Cylindrical Cell Wall Synthesis

The brightly stained transverse bands of Van-FL fluorescence seen with wild-type cells were absent from *ftsZ* and *pbpB* mutants, showing that these bands were due to division-dependent PG synthesis. However, the helical pattern was not affected by these mutations. Therefore, there are at least two spatially specialized PG synthesizing systems in *B. subtilis*. Since MreB and Mbl were both apparently required for cell shape and both make helical cables (Jones et al., 2001), we expected that both proteins would contribute to the helical staining pattern. Surprisingly, based on the effects of the mutants (Figure 2), it appears that cylindrical wall growth is mainly, or exclusively, the function of *mbl* and that in the absence of Mbl protein the cells grow only from polar zones, which probably correspond to ongoing or old division sites. This mode of growth could readily explain both the slow growth of *mbl* mutants and their reduced ability to grow in a straight line. In support of the notion of polar growth, we showed that the *mbl* mutant phenotype is greatly exacerbated and growth virtually stops in cells impaired in division (Figure 3). Genetic crosses involving *mbl* null mutations are characterized by a very poor recovery of transformants and by the appearance among the progeny of a number of different colony variants (Abhayawardhane and Stewart, 1995, R.A.D., unpublished data). We suggest that in otherwise wild-type cells transformed with an *mbl* mutation, the initial transformants have very poor growth but that some acquire mutations that allow the establishment of a new mode of polar growth that is dependent on the division machinery. Conceivably, it involves preventing the normal shut down of PG synthesis at the new cell poles when division has been completed.

The complete dependence of cylindrical wall extension on *mbl* raises interesting questions about the role of *mreB*. One possibility would be that it has a role at the division site, which somehow exerts control over cell width.

General Implications for Bacterial Cell Morphogenesis

The models shown in Figure 5 illustrate how three of the bacteria that we have examined use different strategies of control over growth zones to achieve their partic-

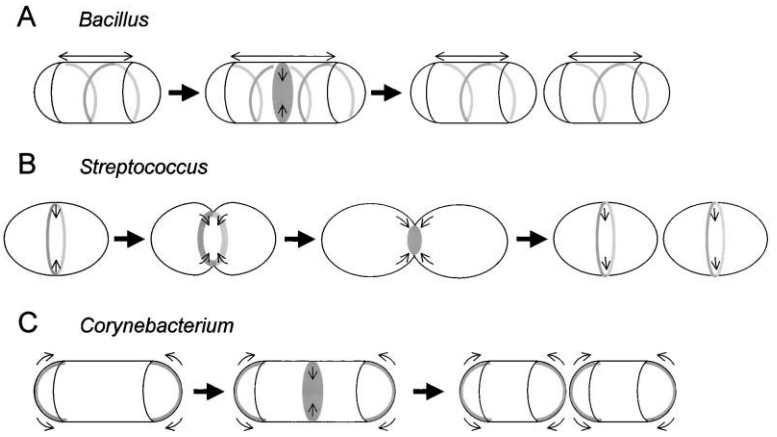

Figure 5. Models for the Different Growth Modes of Diverse Gram-Positive Bacteria

Gray lines and ovals show the sites of nascent wall synthesis during cell elongation and division. Light and dark gray provide perspective, with dark gray at the front of the cell and light at the back. Arrows show the directions of cell elongation or division driven by the wall synthesis. See Discussion for a full description.

ular forms. In *B. subtilis* (Figure 5A), most elongation is generated by Mbl-directed dispersed helical insertion of wall material throughout the cell cylinder, resulting in rapid cylindrical extension. The rate of elongation can increase exponentially in proportion to the surface area of the cylinder. Wall synthesis at the division site is rapid and restricted to a narrow time frame during which a flat, circular disk of material is made. After the poles stretch into their finished hemispherical shape, they are effectively inert. In *Streptococcus* (Figure 5B), there is no MreB cytoskeleton and all wall growth is directed by the division machinery. Division is protracted compared with *B. subtilis*, and closure of the division site is accompanied by elongation from the division site to give a gradually constricting tube. At the end of the division process, synthesis directed by the division machinery is shut down and the newly formed cell poles are inert, so growth is completely dependent on the formation of a new division site. In *Corynebacterium* (Figure 5C), there is no MreB cytoskeleton, but the cells nevertheless acquire a pseudo-rod shape. Here, wall synthesis is again directed by the division machinery initially, but unlike wild-type *B. subtilis* and *Streptococcus*, growth continues indefinitely from the cell poles and, unlike *Bacillus*, it is the cylindrical part of the cell that becomes inert. According to this model, *Corynebacterium glutamicum* and its relatives achieve a rod shape by allowing the growth zone governed by their division machinery to remain active after division. The cell then elongates from its new pole (as well as from its old pole) in the form of a slightly irregular tube. An important principle that emerges here is that morphogenesis of the bacterial cell can be modulated not only by the establishment of new zones of wall growth but also by controlled shut down of growth after division.

What are the advantages and disadvantages of the different modes of rod-shaped growth? First, it seems likely that polar growth is intrinsically slower than dispersed insertion. This could help to explain why the *Mycobacterium/Corynebacterium* group of organisms are relatively slow growing. Polar growth allows only a linear rate of length increase, because growth is restricted to a single zone of constant dimensions at the pole. In contrast, dispersed (helical) growth all over the cylinder (as in *Bacillus*) allows an exponential increase in length because each incremental increase in cylinder length allows a proportionate increase in the rate at which new material can be inserted per cell.

On the other hand, the polar mode of growth may have advantages in terms of the general stability of the PG. *B. subtilis* cells are well known to be susceptible to lysis, due to their autolytic enzymes, which are continuously active throughout the cell cyclinder during elongation. Presumably, there is no such autolytic activity in the cylindrical part of the corynebacterial cell. Moreover, elimination of autolytic turnover in the recently synthesized PG may have been important in evolution of the *Corynebacterium/Mycobacterium* group. These organisms possess a range of cell envelope modifications and additions, such as the insertion of complex lipids (e.g., mycolic acids), that contribute to their tough, resistant character (Chatterjee, 1997). Evolution of such modifications might only have been possible in the context of a wall that was not subject to constant turnover.

To conclude, Van-FL staining provides a powerful probe with which to study the topology of wall synthesis in a range of bacteria. In combination with other rapidly developing cytological methods (Shapiro and Losick, 2000; Errington, 2003) and the information from comparative genomics, the next few years should see considerable progress in understanding the molecular basis of bacterial morphogenesis and its evolution.

Experimental Procedures

Bacterial Strains

B. subtilis strains are described in Table 3. *Streptococcus pneumoniae* R6, *Streptomyces coelicolor* M145, and *Corynebacterium glutamicum* NCIMB 10025 were obtained from B.G. Spratt, K. Flärdh, and NCIMB, respectively.

Growth Conditions

Strains of *Bacillus subtilis* and *Streptomyces coelicolor* were grown in S medium (Sharpe et al., 1998) at 30°C, except in the case of the MreB-depletion experiment, in which CH medium (Partridge and Errington, 1993) was used. Generally, overnight cultures were diluted 1/20 in fresh medium and incubated for 2–3 hr to reestablish exponential growth in the cultures prior to manipulation. *Streptomyces* cultures were initiated by the addition of spores to S medium at 30°C. 2–5 hr after inoculation, the spores were found to have generated relatively short hyphal structures. Extended incubation tended to result in large three-dimensional structures that were impossible to observe by microscopy. *Streptococcus pneumoniae* was grown at 37°C in Todd Hewitt Medium supplemented with BSA. *Corynebacterium glutamicum* was grown at 30°C in PAB overnight,

Table 3. *B. subtilis* Strains

Strain	Genotype	Reference
168	*trpC2*	Laboratory stock
853	*trpC2* P_{spac}*-murE*	This paper
1801	*trpC2 chr::*pJSIZΔpble (P_{spac}*-ftsZ ble*)	Marston et al., 1998
2060	*trpC2* Ω(*amyE::*P_{xyl}*-c-myc-mreBCD spc)* Ω(*mreB::neo*)	Jones et al., 2001
2505	*trpC2* Ω(*mbl::spc*)	Jones et al., 2001
3295	*trpC2 pbpB'::lacI aph-A3* P_{spac}*-pbpB*	This paper
3296	*trpC2* Ω(*mbl::spc*) *chr::*pJSIZΔpble (P_{spac}*-ftsZ ble*)	This paper

then diluted as above and allowed to grow for a further 1–2 hr before staining.

Preparation of Van-FL

A 500 μl amount of vancomycin (Sigma; 10 mg/ml in water) was mixed with 50 μl of 5 (6)-carboxyfluorescein-N-hydroxysuccinimide ester (FLUOS, Roche; 5 mg/ml in DMSO) to give a 5-fold excess of Vancomycin over reactive fluorescein. The reaction was incubated overnight at 4°C and then mixed with 450 μl Tris (pH 8) and incubated for 1 hr further at 22°C. The resulting solution was then stored at −20°C in aliquots of 50 μl. The final concentration of vancomycin in this stock was assumed to be 5 mg/ml with relatively little free fluorescein. The MIC of the Van-FL was almost identical to that of the original vancomycin stock (about 1 μg/ml).

Van-FL Staining

Van-FL was added to growing cultures to a final concentration of 1 μg/ml. The culture was then incubated for 10–20 min to allow absorption of the antibiotic. The cells were then either viewed directly by microscopy or fixed for examination at a later time. For fixation a sample of cells from the culture were washed in PBS, then suspended in 1.6% formaldehyde (in PBS) and left on ice for 1 hr. The fixed cells were washed three times with PBS and then mounted on slides as described previously (Harry and Wake, 1997).

Similar results were obtained using commercially prepared fluorescent vancomycin (Molecular Probes), except that for optimal staining the fluorescent vancomycin needed to be mixed with an equal amount of unlabeled vancomycin. The final vancomycin/Van-FL concentration was again 1 μg/ml.

Microscopic Imaging

For unfixed cells stained with Van-FL, a 2 μl sample of the culture was placed on a microscope slide, covered with a glass cover slip, and viewed directly by epifluorescence microscopy. A similar procedure was used for fixed cells except that the slides were pretreated with polylysine, and the cell sample was allowed to dry onto the slide. The cells were then mounted in 50% glycerol. Images were taken using a Sony CoolSnap HQ cooled CCD camera (Roper Scientific Ltd) attached to a Zeiss Axiovert microscope. The digital images were analyzed with Metamorph version 4.6.9, and the final figures were generated by Adobe Photoshop version 6.

Lysozyme/Detergent Extraction of Van-FL

An overnight culture of strain 168 grown in S medium was diluted to an OD of 0.05 in the same medium and incubated at 30°C until an OD_{600} of 0.5 was reached. Van-FL was then added to a final concentration of 1 μg/ml and the culture was incubated for 20 min further. The cells were then harvested by centrifugation, and the cell pellet was washed twice with PBS. The resulting cell pellet was suspended in 6 ml PBS and divided into two aliquots. One aliquot was then treated with lysozyme and DNase (Sigma) (final concentrations of 500 μg/ml and 1 μg/ml, respectively), then the sample was briefly sonicated (3 × 12 s bursts) and incubated for 5 min at 37°C to lyse the cells (efficient lysis was confirmed by microscopic examination of the sample). The cell lysate was then centrifuged at 180,000 × g for 20 min and a 200 μl aliquot of the supernatant was retained for analysis. The insoluble material was then suspended in 3 ml of PBS and the centrifugation was repeated, after which 200 μl of the supernatant again retained. Finally, the pellet was suspended in 2.7 ml PBS, to which was added 300 μl 10% sodium lauroyl sarcosinate solution (BDH) and held on ice for 10 min with intermittent mixing. This suspension was then centrifuged as before and a sample of the supernatant was retained.

The second cell aliquot was directly resuspended in PBS with sodium lauroyl sarcosinate, sonicated (3 × 12 s bursts), and then held on ice for 10 min with intermittent mixing. The cell suspension was then centrifuged and a sample of the supernatant was retained. The cell pellet was then washed with PBS, centrifuged, and the supernatant was sampled (200 μl). The resulting cell pellet was then suspended in 3 ml PBS containing 500 μg/ml lysozyme and incubated at 37°C for 10 min. Complete lysis was confirmed by microscopy. The suspension was centrifuged at high speed, as above, and a sample was retained. The remaining insoluble material was suspended in PBS containing 1% sodium lauroyl sarcosinate and vortexed prior to high-speed centrifugation to give the final supernatant for sampling.

The quantity of Van-FL in various supernatants was compared to that in the initial sample of the cellular material (solubilised in lysozyme and 0.05% sodium lauroyl sarcosine) as determined by spectrophotometry (excitation at 485 nm; emission at 520 nm) in a BMG spectrofluorimeter.

Acknowledgments

This work was supported by grants from the Biotechnology and Biological Sciences Research Council. J.E. gratefully acknowledges receipt of a BBSRC Senior Research Fellowship. We thank Rut Carballido-López and Christopher J. Schofield for helpful discussions.

Received: January 7, 2003
Revised: April 21, 2003
Accepted: May 8, 2003
Published: June 12, 2003

References

Abhayawardhane, Y., and Stewart, G.C. (1995). *Bacillus subtilis* possesses a second determinant with extensive sequence similarity to the *Escherichia coli mreB* morphogene. J. Bacteriol. *177*, 765–773.

Archibald, A.R., Hancock, I.C., and Harwood, C.R. (1993). Cell wall structure, synthesis, and turnover. In *Bacillus subtilis* and Other Gram-Positive Bacteria: Biochemistry, Physiology, and Molecular Genetics, A.L. Sonenshein, J.A. Hoch, and R. Losick, eds. (Washington, D.C.: American Society for Microbiology), pp. 381–410.

Burman, L.G., Raichler, J., and Park, J.T. (1983). Evidence for diffuse growth of the cylindrical portion of the *Escherichia coli* murein sacculus. J. Bacteriol. *155*, 983–988.

Carballido-López, R., and Errington, J. (2003). The bacterial cytoskeleton: in vivo dynamics of the actin-like protein Mbl of *Bacillus subtilis*. Dev. Cell *4*, 19–28.

Chatterjee, D. (1997). The mycobacterial cell wall: structure, biosynthesis and sites of drug action. Curr. Opin. Chem. Biol. *1*, 579–588.

Clarke-Sturman, A.J., Archibald, A.R., Hancock, I.C., Harwood, C.R., Merad, T., and Hobot, J.A. (1989). Cell wall assembly in *Bacillus subtilis*: partial conservation of polar wall material and the effect of growth conditions on the pattern of incorporation of new material at the polar caps. J. Gen. Microbiol. *135*, 657–665.

Daniel, R.A., and Errington, J. (1993). DNA sequence of the *murE-murD* region of *Bacillus subtilis* 168. J. Gen. Microbiol. *139*, 361–370.

Daniel, R.A., Harry, E.J., and Errington, J. (2000). Role of penicillin-binding protein PBP 2B in assembly and functioning of the division machinery of *Bacillus subtilis*. Mol. Microbiol. *35*, 299–311.

de Pedro, M.A., Quintela, J.C., Höltje, J.V., and Schwarz, H. (1997). Murein segregation in *Escherichia coli*. J. Bacteriol. *179*, 2823–2834.

Doyle, R.J., Chaloupka, J., and Vinter, V. (1988). Turnover of cell walls in microorganisms. Microbiol. Rev. *52*, 554–567.

Errington, J. (2003). Dynamic proteins and a cytoskeleton in bacteria. Nat. Cell Biol. *5*, 175–178.

Foster, S.J., and Popham, D.L. (2001). Structure and synthesis of cell wall, spore cortex, teichoic acids, S-layers, and capsules. In *Bacillus subtilis* and Its Relatives: From Genes to Cells, L. Sonenshein, R. Losick, and J.A. Hoch, eds. (Washington, D.C.: American Society for Microbiology), pp. 21–41.

Ge, M., Chen, Z., Onishi, H.R., Kohler, J., Silver, L.L., Kerns, R., Fukuzawa, S., Thompson, C., and Kahne, D. (1999). Vancomycin derivatives that inhibit peptidoglycan biosynthesis without binding D-Ala-D-Ala. Science *284*, 507–511.

Goffin, C., and Ghuysen, J.M. (1998). Multimodular penicillin-binding proteins: an enigmatic family of orthologs and paralogs. Microbiol. Mol. Biol. Rev. *62*, 1079–1093.

Gray, D.I., Gooday, G.W., and Prosser, J.I. (1990). Apical hyphal extension in *Streptomyces coelicolor* A3(2). J. Gen. Microbiol. *136*, 1077–1084.

Harry, E.J., and Wake, R.G. (1997). The membrane-bound cell division protein DivIB is localized to the division site in *Bacillus subtilis*. Mol. Microbiol. *25*, 275–283.

Henriques, A.O., De Lencastre, H., and Piggot, P.J. (1992). A *Bacillus subtilis* morphogene cluster that includes *spoVE* is homologous to the *mra* region of *Escherichia coli*. Biochimie *74*, 735–748.

Höltje, J.V. (1998). Growth of the stress-bearing and shape-maintaining murein sacculus of *Escherichia coli*. Microbiol. Mol. Biol. Rev. *62*, 181–203.

Jones, L.J.F., Carballido-López, R., and Errington, J. (2001). Control of cell shape in bacteria: helical, actin-like filaments in *Bacillus subtilis*. Cell *104*, 913–922.

Koch, A.L. (1988). Biophysics of bacterial walls viewed as stress-bearing fabric. Microbiol. Rev. *52*, 337–353.

Koch, A.L. (1990). The relative rotation of the ends of *Bacillus subtilis* during growth. Arch. Microbiol. *153*, 569–573.

Koch, A.L. (2000). The bacterium's way for safe enlargement and division. Appl. Environ. Microbiol. *66*, 3657–3663.

Marston, A.L., Thomaides, H.B., Edwards, D.H., Sharpe, M.E., and Errington, J. (1998). Polar localization of the MinD protein of *Bacillus subtilis* and its role in selection of the mid-cell division site. Genes Dev. *12*, 3419–3430.

Mendelson, N.H. (1976). Helical growth of *Bacillus subtilis*: a new model of cell growth. Proc. Natl. Acad. Sci. USA *73*, 1740–1744.

Merad, T., Archibald, A.R., Hancock, I.C., Harwood, C.R., and Hobot, J.A. (1989). Cell wall assembly in *Bacillus subtilis*: visualization of old and new wall material by electron microscopic examination of samples stained selectively for teichoic acid and teichuronic acid. J. Gen. Microbiol. *135*, 645–655.

Michaud, C., Mengin-Lecreulx, D., van Heijenoort, J., and Blanot, D. (1990). Over-production, purification and properties of the uridine-diphosphate-N-acetylmuramoyl-L-alanyl-D-glutamate: meso-2,6-diaminopimelate ligase from *Escherichia coli*. Eur. J. Biochem. *194*, 853–861.

Mobley, H.L.T., Koch, A.L., Doyle, R.J., and Streips, U.N. (1984). Insertion and fate of the cell wall in *Bacillus subtilis*. J. Bacteriol. *158*, 169–179.

Partridge, S.R., and Errington, J. (1993). The importance of morphological events and intercellular interactions in the regulation of prespore-specific gene expression during sporulation in *Bacillus subtilis*. Mol. Microbiol. *8*, 945–955.

Pooley, H.M. (1976a). Layered distribution, according to age, within the cell wall of *Bacillus subtilis*. J. Bacteriol. *125*, 1139–1147.

Pooley, H.M. (1976b). Turnover and spreading of old wall during surface growth of *Bacillus subtilis*. J. Bacteriol. *125*, 1127–1138.

Prescott, L.M., Harley, J.P., and Klein, D.A. (1999). Microbiology, Fourth Edition (Boston: McGraw-Hill).

Reynolds, P.E. (1989). Structure, biochemistry and mechanism of action of glycopeptide antibiotics. Eur. J. Clin. Microbiol. Infect. Dis. *8*, 943–950.

Schlaeppi, J.M., Pooley, H.M., and Karamata, D. (1982). Identification of cell wall subunits in *Bacillus subtilis* and analysis of their segregation during growth. J. Bacteriol. *149*, 329–337.

Shapiro, L., and Losick, R. (2000). Dynamic spatial regulation in the bacterial cell. Cell *100*, 89–98.

Sharpe, M.E., Hauser, P.M., Sharpe, R.G., and Errington, J. (1998). *Bacillus subtilis* cell cycle as studied by fluorescence microscopy: constancy of the cell length at initiation of DNA replication and evidence for active nucleoid partitioning. J. Bacteriol. *180*, 547–555.

Sheldrick, G.M., Jones, P.G., Kennard, O., Williams, D.H., and Smith, G.A. (1978). Structure of vancomycin and its complex with acetyl-D-alanyl-D-alanine. Nature *271*, 223–225.

Stone, K.J., and Strominger, J.L. (1971). Mechanism of action of bacitracin: complexation with metal ion and C 55 -isoprenyl pyrophosphate. Proc. Natl. Acad. Sci. USA *68*, 3223–3227.

Trachtenberg, S. (1998). Mollicutes-wall-less bacteria with internal cytoskeletons. J. Struct. Biol. *124*, 244–256.

Umeda, A., and Amako, K. (1983). Growth of the surface of *Corynebacterium diphtheriae*. Microbiol. Immunol. *27*, 663–671.

van den Ent, F., Amos, L.A., and Löwe, J. (2001). Prokaryotic origin of the actin cytoskeleton. Nature *413*, 39–44.

Vuorio, R., and Vaara, M. (1992). Mutants carrying conditionally lethal mutations in outer membrane genes *omsA* and *firA* (*ssc*) are phenotypically similar, and *omsA* is allelic to *firA*. J. Bacteriol. *174*, 7090–7097.

Wientjes, F.B., and Nanninga, N. (1989). Rate and topography of peptidoglycan synthesis during cell division in *Escherichia coli*: concept of a leading edge. J. Bacteriol. *171*, 3412–3419.

Woldringh, C.L., Huls, P., Pas, E., Brakenhoff, G.J., and Nanninga, N. (1987). Topography of peptidoglycan synthesis during elongation and polar cap formation in a cell division mutant of *Escherichia coli* MC4100. J. Gen. Microbiol. *133*, 575–586.